Mechanics & Industry **26**, 6 (2025)

https://doi.org/10.1051/meca/2024040

Mechanics & Industry

Available online at:
www.mechanics-industry.org

ORIGINAL ARTICLE OPEN ACCESS

On modelling of the one dimensional pseudoelastic effect of shape memory alloys

Imade Zidane* and Belkacem Meddour

Laboratory of Engineering and Sciences of Advanced Materials (ISMA), Department of Mechanical Engineering, ABBES LAGHROUR University Khenchela, Algeria

Received: 27 August 2024 / Accepted: 31 December 2024

Abstract. Last decades, a qualitative leap in materials engineering was observed, through developing new materials or discovering new properties. The shape memory alloys are a group of materials exhibiting singular behaviour under a coupled thermomechanical loading, and they are widely used in numerous applications because of their properties. To exploit these properties in engineering, several constitutive models of were developed. The aim of this work is to build a constitutive model that could describe the pseudoelastic behaviour of shape memory alloys in a simpler and more accurate way. Based on thermodynamics and mechanics laws and principles, the developed constitutive model was implemented in an algorithm and compared with experimental data in order to assess its accuracy. The obtained results indicated that the agreement between the real and computer-simulated stress-strain curves was good. This reaffirmed the model's ability to predict the pseudoelastic behaviour of the shape memory materials under various loading states. These results thus validate especially the temperature sensitivity of Nitinol alloys, which should be taken into account when designing devices that need to function reliably.

Keywords: Pseudoelasticity / memory / thermomechanical / transformation / fraction

1 Introduction

The basic materials that go into making modern technology are what drive its progress. The advancement of technology can benefit from a wide variety of materials. Among these categories are smart materials, which are recognized for exhibiting a variety of distinct properties in contrast to other kinds of materials [1].

Lightweight and flexible systems are becoming more and more in demand in structural engineering, robotics, and aerospace, where the emergence of smart materials and structures is transforming design ideas [2].

Different smart or responsive materials are utilized in the modern era of technology. These materials can change their structure, size, or mechanical qualities in response to external stimuli, such as a certain level of mechanical stress, pressure, temperature, pH, or UV radiation. As the world's temperatures rise and weather patterns grow more severe and unpredictable [3].

Shape memory alloys, sometimes known as SMAs, are among the greatest kinds of smart materials. They have been the focus of much commercial and scientific attention since their discovery in the early 1930s [4].

Moreover shape memory alloys constitute a unique class of multifunctional materials that can change their behavior in response to mechanical or thermal stimulation are now widely used in a variety of applications [5,7].

The majority of research on shape memory alloys (SMAs) has been done with NiTi SMA. It should be noticed that before the discovery of the shape memory effect (SME) in a nickel-titanium (NiTi), by William Buehler and Frederick Wang in 1962, the importance and the demand of SMAs for most engineering and technical applications was not positively realized, it is the most well-known SMA [8,9].

NiTi shape-memory alloys have found extensive application in industries like electronic equipment, aircraft, and biomedicine military applications, telecommunications, and industrial process control, technical applications because of their exceptional form recovery qualities, including the pseudoelastic effect (PE) and shape memory effect (SME) [10–13].

In addition, shape memory alloy (SMA) offers superior fatigue, corrosion resistance, and high damping in addition to its two distinctive qualities of shape memory and superelasticity. As a result, SMA is frequently utilized for vibration control and reinforcing in the field of civil engineering. It is distinguished by its low modulus of elasticity, moderate density, reasonable impact resistance and ductility, high strength at room temperature and raised temperatures, and biocompatibility that is susceptible to changes in temperature and composition [14,15].

* e-mail: Zidane.imade@univ-khenchela.dz

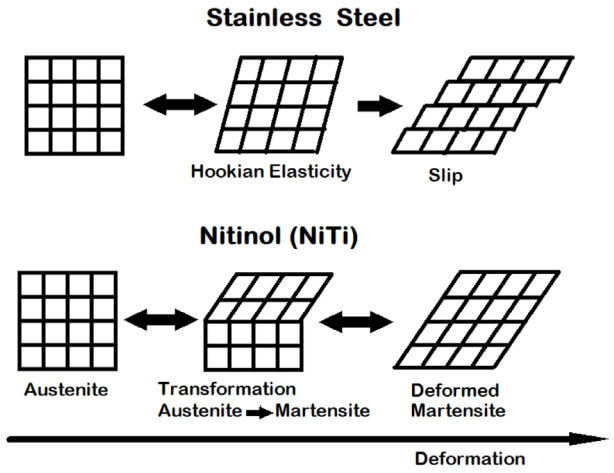

Fig. 1. Schematic presentation of lattice structure changes caused by applied stress in stainless steel or nitinol [18].

Even though having outstanding mechanical properties, NiTi SMAs have limited uses due to their high material cost and challenging metal formation [16].

The widespread use of conventional materials has been made possible by their well-known behavior, but novel uses in the medical and aerospace fields have been made possible by the discovery of new features resulting from the unique behavior of materials known as shape memory alloys. Scientists and academics have paid close attention to this peculiar behavior. As a result, several models were put forth. These models are expanded versions of common materials based on framework theories and the laws of thermodynamics [17].

There are two phases in these materials: the austenite phase and the martensite phase. SMAs undergo phase transitions, going from the austenite to the martensite and back again.

The elastic (reversible) response to an applied stress produced by a phase transition between a SMA's austenite and martensite phases is called superelasticity (SE), sometimes known as pseudoelasticity. Pseudoelasticity, in contrast to the shape memory effect, occurs independently of temperature. SE occurs at a high enough temperature where the alloy is in its parent phase and its original shape and there is a stable austenite phase. An austenite phase may be stimulated to change into a stable, detwinned martensite phase also referred to as "stress-induced martensite" by applying a mechanical strain. This strain is accommodated by the immediate regions related shear.

Compared to conventional elastic deformation, which can only handle strains of up to around 0.5% for most metals, NiTi SMAs allow for relatively significant strains of up to 8% without plastic deformation. However, martensitic phase changes must account for all of the deformation in order for this phenomena to occur. It is possible that some traditional plastic flow (dislocation glide) will occur if an extreme strain is applied, and the process will be irreversible (Fig. 1) [19,20].

Note that these materials have a very basic use: they can be easily deformed by applying an external force, and when heated over a specific temperature either internally or externally they will contract or return to their original shape (For example Joule heating in case of some applications) [21].

The effect of pseudoelasticity, on which we focused in this work, is the ability of SMA to deform in large proportions and to recover their initial configuration upon unloading. This behaviour is observable when an increasing stress is applied to a volume of SMA, in quasi-isothermal conditions, from a totally austenitic state, i.e. when the test temperature $T > A_s^0$ (Figs. 2 and 3).

The application of a stress causes the elastic deformation of the austenite, followed by the martensitic transformation from the martensite start stress σ_{Ms} up to the martensite finish stress σ_{Mf} where all the austenite is transformed into martensite. During unloading, the martensite deforms elastically up to the austenite start stress σ_{As} from which the austenitic transformation begins which ends as soon as the stress $\sigma < \sigma_{\mathrm{Af}}$.

In this paper, the work focused on the pseudoelastic effect, a constitutive model was built and the algorithm was developed using MATLAB. The experimental data were supplied by obtained results through the study of Ng et al. [23].

2 Methods and materials

2.1 Constitutive equations

First of all let us consider a representative elementary volume (Fig. 4)

Fraction of martensite is given by:

$$f = \frac{V_M}{V_A + V_M}. \tag{1}$$

The thermodynamic potential used in this work is Gibbs free energy density, which is denoted FED (Free Energy Density) can be written as [22,24]:

$$FED(\sigma, T, f) = -\frac{\sigma^2}{2}.\left[\frac{1-f}{E_A} + \frac{f}{E_M}\right] - \sigma \cdot f \cdot \varepsilon^0 + B \cdot f \cdot (f+1) \cdot \left(T - T^0\right) + C \cdot f \cdot (f-1) \tag{2}$$

$\frac{\sigma^2}{2}.\left[\frac{1-f}{E_A} + \frac{f}{E_M}\right]$: Elastic energy of deformation; $\sigma \cdot f \cdot \varepsilon^0$: Mechanical work associated with the transformation of martensite; $B \cdot f \cdot (f+1) \cdot (T - T^0)$: Free energy of phase change; $C \cdot f \cdot (f-1)$: Energy of interaction between martensite and austenite; E_A and E_M: Young modulus respectively of austenite and martensite; ε^0: Maximum deformation along an axis; T^0: Reference temperature; B and C: Constants to be determined.

The dissipation occurring during the transformation leads to consider Clausius inequality:

$$-\frac{\partial FED}{\partial f}.\frac{df}{dt} \geq 0. \tag{3}$$

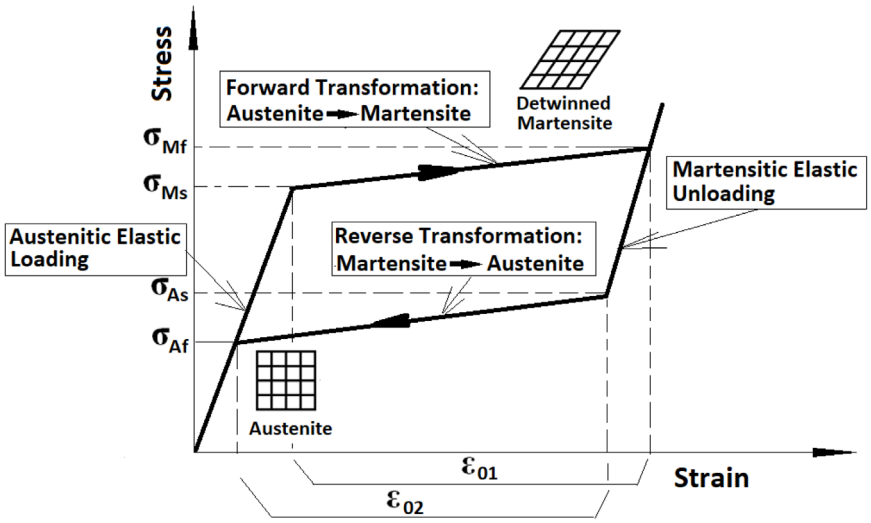

Fig. 2. Diagram illustrating pseudoelasticity effect [22].

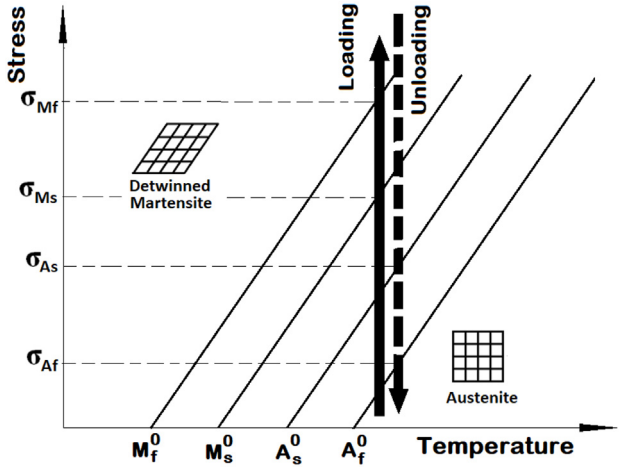

Fig. 3. Path of loading [22]. σ_{MS}: Martensite start stress; σ_{Mf}: Martensite finish stress; σ_{AS}: Austenite start stress; σ_{Af}: Austenite finish stress; M_s^0: Martensite temperature start (Zero-stress); M_f^0: Martensite temperature finish (Zero-stress); A_s^0: Austenite temperature start (Zero-stress); A_f^0: Austenite temperature finish (Zero-stress); ε_{01}: Maximum strain in forward transformation; ε_{02}: Maximum strain in reverse transformation.

Driving force, deriving from the thermodynamic potential FED is given by:

$$-\frac{\partial FED}{\partial f} = THD^F. \tag{4}$$

Since there is dissipation during the transformation of martensite into austenite (and austenite to martensite as well), it can be assumed that dissipation pseudo-potential exists, denoted PTH^D, then quantified by the suggested expression:

$$PTH^D = -K\left(\frac{f^3}{3} + \frac{f^2}{2}\right) - Hf \tag{5}$$

K and H are constants to be determined.

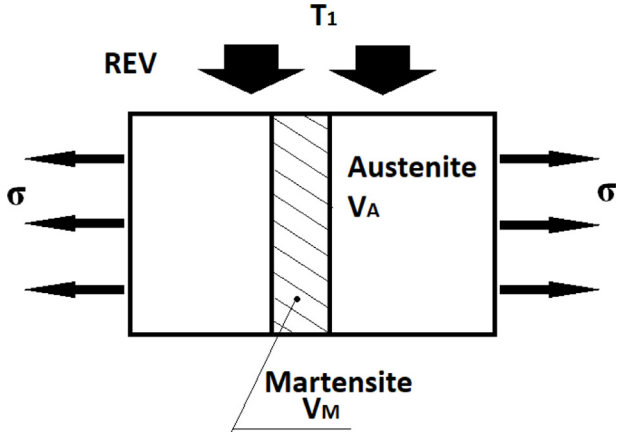

Fig. 4. Representative elementary volume.

Taking into account that dissipative force driving denoted DIS^F is derived from dissipative pseudo-potential PTH^D:

$$-\frac{dPTH^D}{df} = DIS^F. \tag{6}$$

This will give:

$$DIS^F = Kf(f+1) + H. \tag{7}$$

The transformation of austenite into martensite (Forward transformation) occurs when the following condition is satisfied:

$$THD^F = DIS^F. \tag{8}$$

Let us consider the following criteria function denoted Ω^{FOR}:

$$\Omega^{FOR}(\sigma, f, T) = THD^F - DIS^F. \tag{9}$$

Then:

$$\Omega^{FOR}(\sigma,f,T)=\frac{\sigma^2}{2}\cdot\left[\left(\frac{1}{E_M}\right)-\left(\frac{1}{E_A}\right)\right]+\sigma\cdot\varepsilon^0 - B\cdot(2f+1)\cdot\left(T-T^0\right)-C\cdot(2f-1) - K\cdot f\cdot(f+1)-H=0. \quad (10)$$

Since the function $\Omega^{FOR}(\sigma, f, T)$ is zero, it is consistent that its time derivative is also zero:

$$\frac{d\Omega^{FOR}}{dt}=\frac{\partial\Omega^{FOR}}{\partial\sigma}\cdot\frac{d\sigma}{dt}+\frac{\partial\Omega^{FOR}}{\partial T}\cdot\frac{dT}{dt}+\frac{\partial\Omega^{FOR}}{\partial f}\cdot\frac{df}{dt}=0. \quad (11)$$

Then:

$$\left[\sigma\cdot\left(\frac{1}{E_M}-\frac{1}{E_A}\right)+\varepsilon^0\right]\cdot\dot{\sigma}-B\cdot(2f+1)\cdot\dot{T} + \left[-2B\cdot\left(T-T^0\right)-2C-K\cdot(2f+1)\right]\cdot\dot{f}=0. \quad (12)$$

Equation (11) leads to:

$$\dot{f}=\frac{\left[\sigma\cdot\left(\frac{1}{E_M}-\frac{1}{E_A}\right)+\varepsilon^0\right]\cdot\dot{\sigma}-B\cdot(2f+1)\cdot\dot{T}}{-2B\cdot\left(T-T^0\right)-2C-K\cdot(2f+1)} \quad (13)$$

when it comes into isothermal case, equation (12) will be rewritten as following:

$$\dot{f}=\frac{-\left[\sigma\cdot\left(\frac{1}{E_M}-\frac{1}{E_A}\right)+\varepsilon^0\right]\cdot\dot{\sigma}}{-2B\cdot\left(T-T^0\right)-2C-K\cdot(2f+1)}. \quad (14)$$

In case of reverse transformation:

$$THD^F=-DIS^F. \quad (15)$$

The criteria function denoted Ω^{REV} will be written as:

$$\Omega^{REV}(\sigma,f,T)=THD^F+DIS^F. \quad (16)$$

Then

$$\Omega^{REV}(\sigma,T,f)=\frac{\sigma^2}{2}\cdot\left[\left(\frac{1}{E_M}\right)-\left(\frac{1}{E_A}\right)\right]+\sigma\cdot\varepsilon^0 - B\cdot(2f+1)\cdot\left(T-T^0\right)-C\cdot(2f-1) + K\cdot f\cdot(f+1)+H. \quad (17)$$

Similarly to equation (12), the expression of fraction rate is written as following:

$$\dot{f}=\frac{\left[\sigma\cdot\left(\frac{1}{E_M}-\frac{1}{E_A}\right)+\varepsilon^0\right]\cdot\dot{\sigma}-B\cdot(2f+1)\cdot\dot{T}}{-2B\cdot\left(T-T^0\right)-2C+K\cdot(2f+1)}. \quad (18)$$

Table 1. Experimental data ($T=65\,°C$).

σ_{MS} (MPa)	268	E_M (Mpa)	18442
σ_{Mf} (MPa)	275	M_s^0 (K)	279
σ_{AS} (MPa)	62	ε_{10}	0.06106
σ_{Af} (MPa)	37	ε_{02}	0.05903
E_A (MPa)	25775		

Table 2. Parameters of the model.

B (MPa. K $^{-1}$)	0.08491
C (MPa)	–4.53424
K (MPa)	–0.25953
H (MPa)	7.36171

In isothermal case (T = cte):

$$\dot{f}=-\left[\sigma\cdot\left(\frac{1}{E_M}-\frac{1}{E_A}\right)+\varepsilon^0\right]\cdot\frac{\dot{\sigma}}{\left\{-2B\cdot\left(T-T^0\right)-2C+K\cdot(2f+1)\right\}}. \quad (19)$$

2.2 Determination of constants B, C, K and H

The experimental data, were supplied by (Ng et al.) work. They carried out a set of experiments in polycrystalline NiTi shape memory alloy tubes by tensile testing at different temperatures: $T=46\,°C$, $T=56\,°C$, $T=65\,°C$ and $T=70\,°C$ [23].

In order to determine constants B, C, K and H, we used experimental results obtained at $T=65\,°C$ and they are illustrated by Table 1.

The reference temperature was fixed:

$$T^0=M_s^0.$$

At the start of the forward transformation we have the following conditions:

$$\sigma=\sigma_{MS};T=T_1;f=0$$

$$\Omega^{FOR}(\sigma=\sigma_{MS},T=T_1,f=0) =\left(\frac{\sigma_{MS}2}{2}\right)*\left(\frac{1}{E_M}-\frac{1}{E_A}\right)+\sigma_{MS}*\varepsilon_{01}-B *\left(T_1-M_s^0\right)+C-H=0. \quad (20)$$

At the end of forward transformation:

$$\sigma=\sigma_{MF},T=T_1,f=1$$

$$\Omega^{FOR}(\sigma = \sigma_{MF}, T = T_1, f = 1) = \left(\frac{\sigma_{MF}2}{2}\right) * \left(\frac{1}{E_M} - \frac{1}{E_A}\right) + \sigma_{MF} * \varepsilon_{01} - 3B * \left(T_1 - \mathrm{M}_s^0\right) - C - H = 0. \quad (21)$$

At the start of the reverse transformation:

$$\sigma = \sigma_{AS}, T = T_1, f = 1$$

$$\Omega^{REV}(\sigma = \sigma_{AS}, T = T_1, f = 1) = \left(\frac{\sigma_{AS}2}{2}\right) * \left(\frac{1}{E_M} - \frac{1}{E_A}\right) + \sigma_{AS} * \varepsilon_{02} - 3B * \left(T_1 - \mathrm{M}_s^0\right) + 2 * K + H = 0. \quad (22)$$

At the end of the reverse transformation:

$$\sigma = \sigma_{AF}, T = T_1, f = 0$$

$$\Omega^{REV}(\sigma = \sigma_{AF}, T = T_1, f = 0) = \left(\frac{\sigma_{AF}2}{2}\right) * \left(\frac{1}{E_M} - \frac{1}{E_A}\right) + \sigma_{AF} * \varepsilon_{02} - B * \left(T_1 - \mathrm{M}_s^0\right) + C + H. \quad (23)$$

The constants B, C, K and H were computed and put in Table 2.

3 Results and discussion

The algorithm is based on the calculation of criteria function $\boldsymbol{\Omega^{FOR}}$ when it is zero the transformation occurs then an updating of both stress and martensite fraction is achieved, else stress is only updated. The same approach is followed regarding the reverse transformation.

The results obtained, after having performed the simulation, are illustrated by figures (Figs. 3–7).

First of all Figures 5a, 6a, 7a and 8a show the history of the mechanical load for each case of numerical simulation. Figure 5b at $T = 46\,°C$ shows only a gap, because of imperfect austenite elastic behavior of NiTi (Seeming to be related to the existence of the R phase), at the end of austenite elastic loading. The results illustrated by Figures 6b, 7b and 8b are in a good agreement with experimental curves, especially at T=65 °C and above. The evolution of martensite fraction computed and shown in Figures 5c, 6c, 7c and 8c, in addition to being the main indicator of occurring transformation, fits the constitutive model well.

Finally Figure 9 illustrates the ability of the model to respond at any temperature.

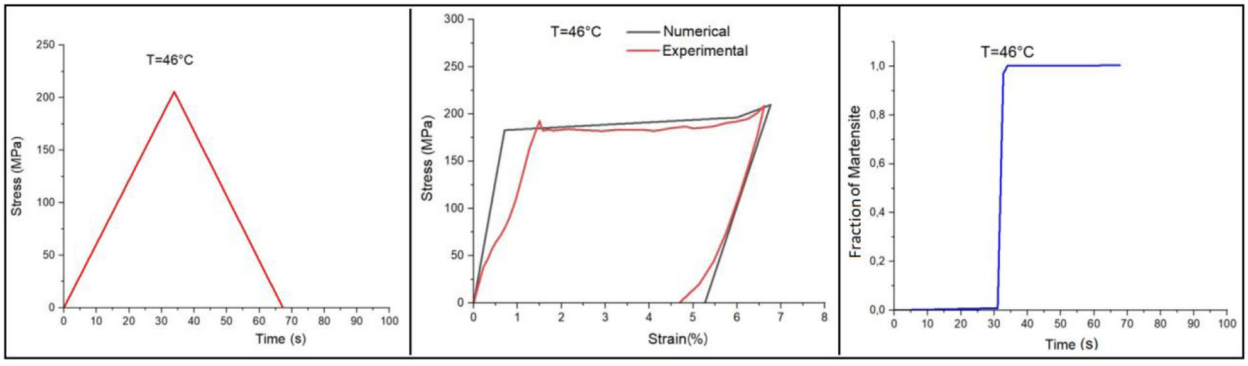

Fig. 5. At $T = 46\,°C$: (a) History of mechanical loading, (b) stress vs strain, (c) evolution of martensite fraction.

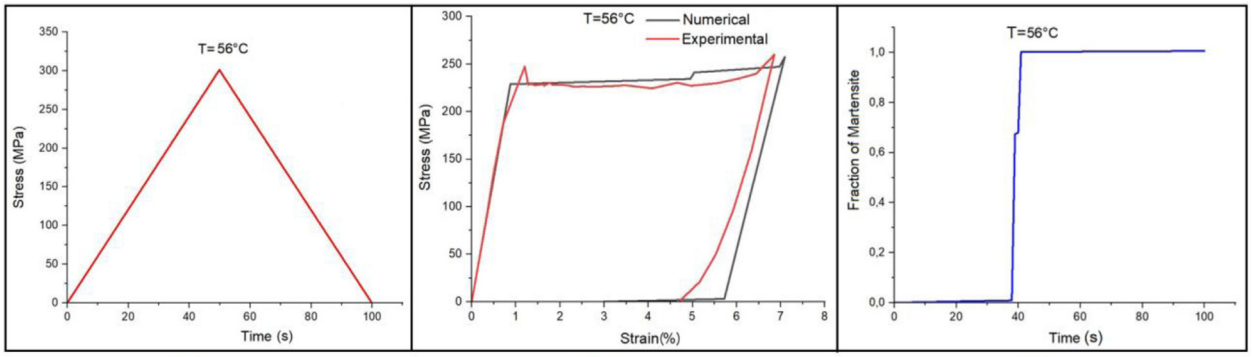

Fig. 6. At $T = 56\,°C$: (a) History of mechanical loading, (b) stress vs strain, (c) evolution of martensite fraction.

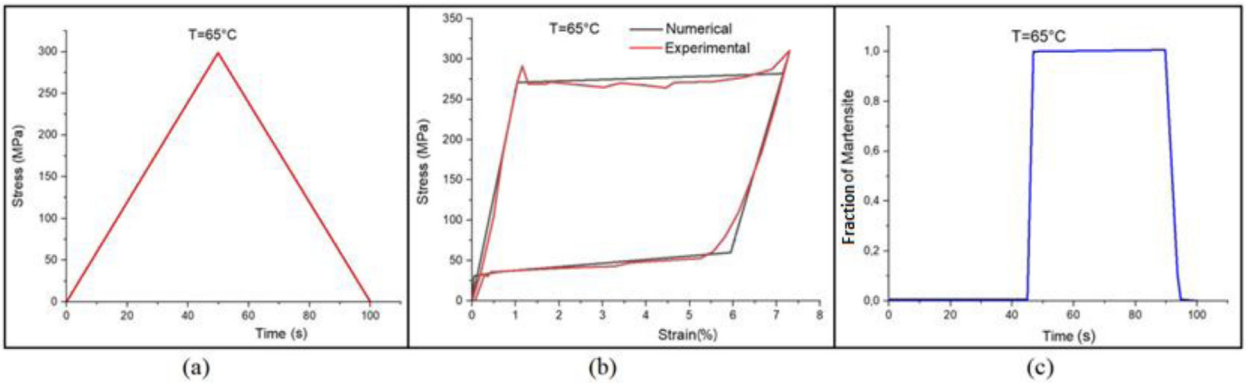

Fig. 7. At $T = 65\,°C$: (a) History of mechanical loading, (b) stress vs strain, (c) evolution of martensite fraction.

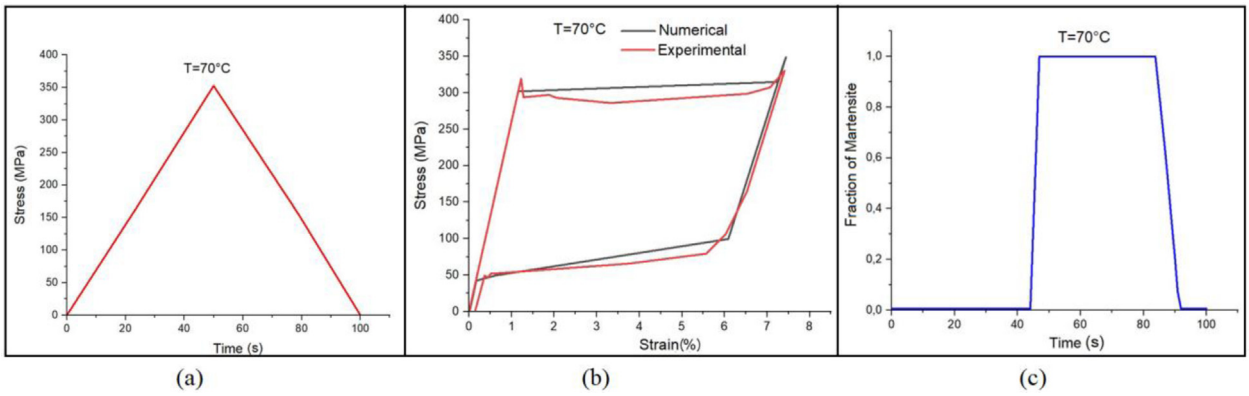

Fig. 8. At $T = 70\,°C$: (a) History of mechanical loading, (b) stress vs strain, (c) evolution of martensite fraction.

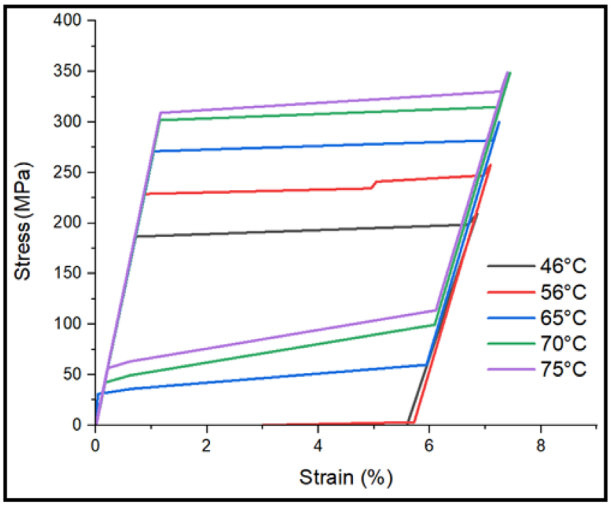

Fig. 9. Response of the model at different temperatures.

4 Conclusion

In this paper, it was focused on the pseudoelasticity effect of shape memory alloys. The constitutive equations were written following mechanics and thermodynamics laws. An algorithm was built and allowed implementing necessary experimental data, the results showed that the model, accurately describes the material's behavior at various temperatures and matches experimental data well.

The model's ability to forecast the pseudoelastic effect in NiTi alloys is strengthened by experimental data, which is important for applications that need precise control over mechanical properties through temperature manipulation.

Funding

None stated.

Conflicts of interest

The authors state no conflict of interest.

Data availability statement

No new data/codes were created or analyzed in this study.

Author contribution statement

The work was distributed between all the authors on this article.

References

[1] B.M. Ibrahım, S.S. Mohammed, E. Balci, A review on comparison between NiTi-based and Cu-based shape memory alloys, J. Phys. Chem. Funct. Mater. **6**, 40–50 (2023)

[2] S. Palaniyappan et al., Surface treatment strategies and their impact on the material behavior and interfacial adhesion strength of shape memory alloy NiTi wire integrated in glass fiber-reinforced polymer laminate structures, Materials **17**, 3513 (2024)

[3] J. Bhattacharjee, S. Roy, Smart materials for sustainable energy, Nat. Resour. Conserv. Res. **7**, 5536 (2024)

[4] M. Vollmer, A. Bauer, T. Niendorf, Combined shape memory alloy phenomena: a novel approach to extend applications of shape memory alloys, Mater. Lett. **347**, 134643 (2023)

[5] N. Lokesh, U.S. Mallik, A.G. Shivasiddaramaiaha, T.N. Mohith, N. Praveen, Characterization and evaluation of shape memory effect of Cu-Zn-Al shape memory alloy, J. Mines Met. Fuels **70**, 324–331 (2022)

[6] A.A. Karakalas, T.T. Machairas, D.C. Lagoudas, D.A. Saravanos, Quantification of shape memory alloy damping capabilities through the prediction of inherent behavioral aspects, Shape Mem. Superelasticity **7**, 7–29 (2021)

[7] N. Farjam, M. Nematollahi, M.T. Andani, M.J. Mahtabi, M. Elahinia, Effects of size and geometry on the thermomechanical properties of additively manufactured NiTi shape memory alloy, Int. J. Adv. Manuf. Technol. **107**, 3145–3154 (2020)

[8] A.S. Hamdy Makhlouf, N.Y. Abu-Thabit, D. Ferretiz, Chapter 12-Shape-memory coatings, polymers, and alloys with self-healing functionality for medical and industrial applications, in *Advances in Smart Coatings and Thin Films for Future Industrial and Biomedical Engineering Applications*, edited by A.S.H. Makhlouf, N.Y. Abu-Thabit (Elsevier, 2020), pp. 335–358

[9] H. Khodaverdi, M. Mohri, E. Ghafoori, A.S. Ghorabaei, M. Nili-Ahmadabadi, Enhanced pseudoelasticity of an Fe-Mn-Si-based shape memory alloy by applying microstructural engineering through recrystallization and precipitation, J. Mater. Res. Technol. **21**, 2999–3013 (2022)

[10] Q. Shen et al., Effect of cold-drawn-induced amorphous phase on microstructure and pseudoelasticity properties of nanocrystalline NiTi alloys, J. Mater. Res. Technol. **26**, 7936–7946 (2023)

[11] Z. Kang, A. Yu, Y. Wang, Y. Qin, Q. Wu, H. Liu, Finite element method of functionally graded shape memory alloy based on UMAT, Mathematics **12**, 282 (2024)

[12] F. Furgiuele, P. Magarò, C. Maletta, E. Sgambitterra, Functional and structural fatigue of pseudoelastic NiTi: global vs local thermo-mechanical response, Shape Mem. Superelasticity **6**, 242–255 (2020)

[13] C. Bouvet, S. Calloch, C. Lexcellent, A phenomenological model for pseudoelasticity of shape memory alloys under multiaxial proportional and nonproportional loadings, Eur. J. Mech. A/Solids **23**, 37–61 (2004)

[14] M. Zhan, J. Liu, D. Wang, X. Chen, L. Zhang, S. Wang, Optimized neural network prediction model of shape memory alloy and its application for structural vibration control, Materials **14**, 6593 (2021)

[15] P. Shabani Nezhad, The effect of microstructural defects and geometrical features on fatigue behavior of superelastic nitinol wires, Diss. 1934(2023). Available: https://epublications.marquette.edu/dissertations_mu/3030

[16] L.-W. Tseng, P.-Y. Lee, N.-H. Lu, Y.-T. Hsu, C.-H. Chen, Shape memory properties and microstructure of FeNiCoAlTaB shape memory alloys, Crystals **13**, 852 (2023)

[17] B. Meddour, H. Zedira, H. Djebaili, One dimensional modeling of the shape memory effect, Model. Numer. Simul. Mater. Sci. **3**, 124–128 (2013)

[18] R.V.R. Kumar, S. Prashantha, S.H. Adarsh, P.C.A. Kumara, A Review Article on FeMnAlNi shape memory alloy, J. Mines Met. Fuels **70(8A)**, 355–359 (2022)

[19] N. Choudhary, D. Kaur, Shape memory alloy thin films and heterostructures for MEMS applications: a review, Sens. Actuators Phys. **242**, 162–181 (2016)

[20] T.W. Duering, D. Stockel, A. Keeley, Actuator and work production devices, in Engineering Aspects of Shape Memory Alloys, edited by T.W. Duering, K.N. Melton, D. Stockel, C.M. Wayman (Butterworth-Helnemann, London, 1990), pp. 181–194

[21] J. Mohd Jani, M. Leary, A. Subic, M.A. Gibson, A review of shape memory alloy research, applications and opportunities, Mater. Des. 1980–2015 **56**, 1078–1113 (2014)

[22] D.C. Lagoudas, Shape Memory Alloys: Modeling and Engineering Applications, Springer-Verlag New York Inc.; 2008th edition (2 July 2008); Springer-Verlag New York Inc

[23] E. Patoor, A. Eberhardt, M. Berveiller, Micromechanical modelling of superelasticity in shape memory alloys, Pitman Res. Notes Math. **296**, 38–54 (1993)

[24] K.L. Ng, Q.P. Sun, Stress-induced phase transformation and detwinning in NiTi polycrystalline shape memory alloy tubes, Mech. Mater. **38**, 41–56 (2006), https://doi.org/10.1016/j.mechmat.2005.05.008

Cite this article as: I. Zidane, M. Belkacem, On modelling of the one dimensional pseudoelastic effect of shape memory alloys, Mechanics & Industry 26, 6 (2025), https://doi.org/10.1051/meca/2024040